Available online at www.sciencedirect.com
ScienceDirect
Journal of the European Ceramic Society 30 (2010) 1659–1667
www.elsevier.com/locate/jeurceramsoc

Fracture toughness of Al_2O_3 fibers with an artificial notch introduced by a focused-ion-beam

S. Ochiai [a,*], S. Kuboshima [a], K. Morishita [b], H. Okuda [a], T. Inoue [c]

[a] *Department of Materials Science and Engineering, Graduate School of Engineering, Kyoto University, Yoshida, Sakyo-ku, Kyoto 606-8510, Japan*
[b] *Institute for Materials Research, Tohoku University, Katahira, 2-chome, Aoba-ku, Sendai 980-8577, Japan*
[c] *Innovative Materials Engineering Laboratory, National Institute for Materials Science (NIMS), Sengen 1-2-1, Tsukuba 305-0047, Japan*

Received 10 September 2009; received in revised form 29 November 2009; accepted 30 December 2009
Available online 8 February 2010

Abstract

The present work was carried out to estimate the fracture toughness of two types of Al_2O_3 fibers ($85Al_2O_3$–$15SiO_2$, Altex® (Sumitomo Chemical Co., Ltd) and α-Al_2O_3, Almax® (Mitsui Mining Co., Ltd)) and to elucidate the transition from the intrinsic defects-induced fracture to introduced notch-induced one. With an application of the focused-ion (Ga^+)-beam micromachining method, a mode I type straight-fronted edge notch with a notch-tip radius around 25 nm was introduced in fiber specimen. The fracture toughness K_{Ic} was estimated for each fiber specimen based on the fracture mechanical approach in which the measured values of notch depth, fiber diameter, fracture strength and calculated correction factor were substituted. The fracture toughness values of the $85Al_2O_3$–$15SiO_2$ and α-Al_2O_3 fibers were estimated to be 1.86 ± 0.24 and 2.05 ± 0.13 MPa $m^{1/2}$, respectively. The fracture toughness value was almost independent of the fiber diameter and notch depth in both fibers tested. From the obtained fracture toughness value and the measured fracture strength of the original fiber, the notch depth at the transition from intrinsic defects-induced fracture to notch-induced one, corresponding to the equivalent size of the intrinsic defects that determines the strength of the original fiber, were estimated to be 0.3 and 0.8 μm for $85Al_2O_3$–$15SiO_2$ and α-Al_2O_3 fibers, respectively.

Keywords: Al_2O_3; Fibers; Fracture; Strength; Toughness and toughening

1. Introduction

The small diameter fibers such as Al_2O_3, SiC and C (carbon) fibers are used as reinforcements for composite materials. For estimation of fracture toughness value of these fibers, the difficulty arises from the small physical dimensions, due to which proper method to introduce small notches is limited. In addition, the fiber diameter is not unique, being different among the test fiber specimens (it has been reported that the diameters of SiC, C and Al_2O_3 fibers are distributed in the range of around 7.5–14,[1–5] 5.1–11[6,7] and 8–17 μm,[1,2,8–10] respectively.) Thus, the influence of the fiber diameter on fracture strength shall be incorporated in estimation of fracture toughness for each fiber test specimen.

Due to the difficulties mentioned above, the fracture toughness has been estimated with the indentation fracture method or the empirical method (hereafter noted simply as mirror zone size method), which uses the relation between the fracture toughness and size of the mirror zone in fracture surface. However, concerning the indentation fracture method, it has been shown that indentation-induced subthreshold flaws on fused silica fibers in an inert environment behave differently from the post-threshold ones, due to which consistent result cannot be obtained for the specimens with different flaw size.[11,12] The mirror zone size method can be applied only to amorphous or amorphous-like fibers that exhibit mirror, mist and hackle zones in fracture surface, but not to crystalline fibers that do not show such zones.

Thus there is a need to develop a method to introduce a sharp artificial notch directly in the small diameter crystalline fibers for estimation of fracture toughness. In our preceding work,[13] it was attempted to introduce a sharp artificial notch in small diameter fiber with a focused-ion-beam (FIB). With this method, a

* Corresponding author. Tel.: +81 75 753 4834; fax: +81 75 753 4841.
E-mail address: shojiro.ochiai@materials.mbox.media.kyoto-u.ac.jp (S. Ochiai).

0955-2219/$ – see front matter © 2010 Elsevier Ltd. All rights reserved.
doi:10.1016/j.jeurceramsoc.2009.12.020

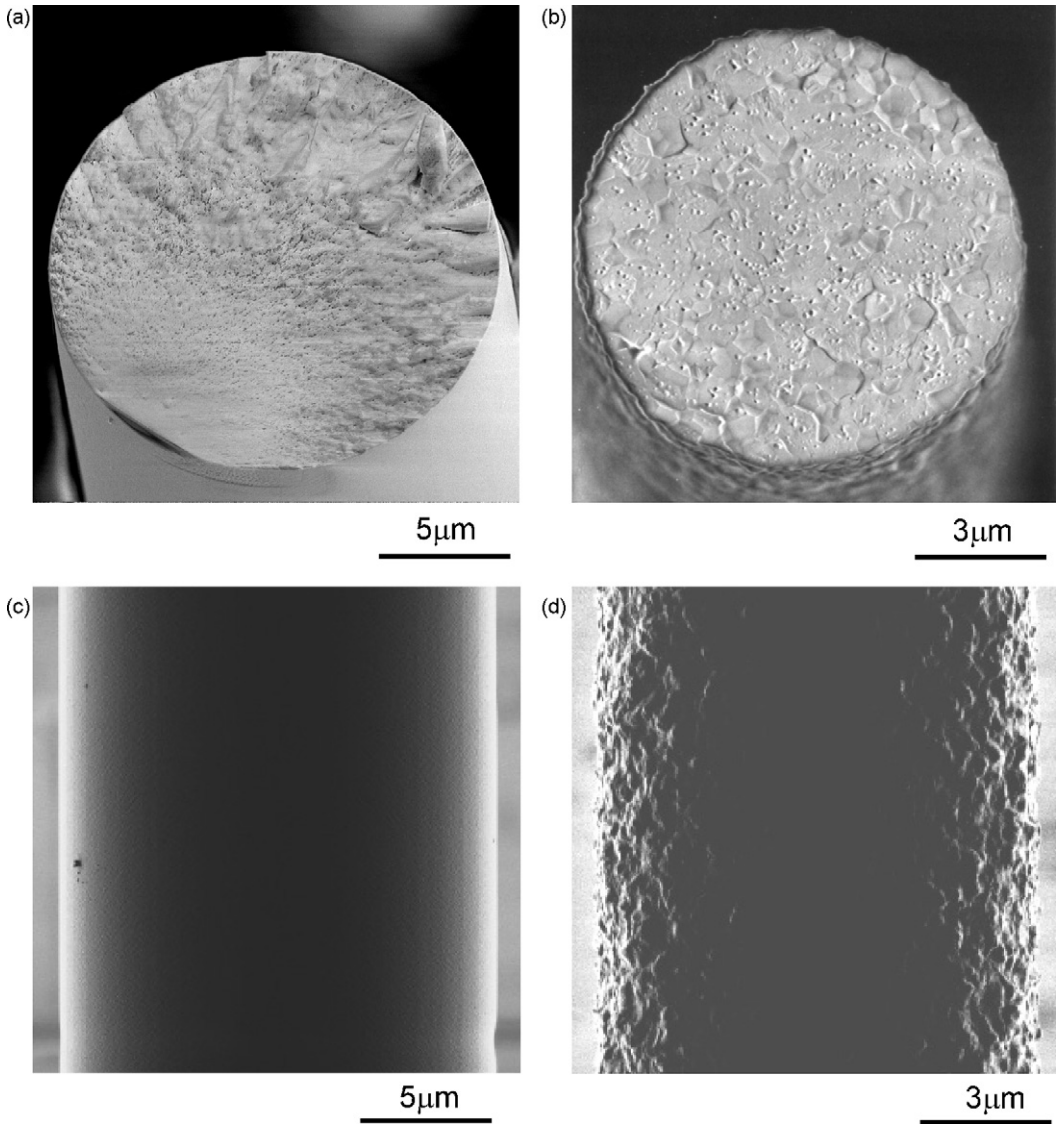

Fig. 1. Fracture surface of the unnotched (a) $85Al_2O_3$–$15SiO_2$ and (b) α-Al_2O_3 fiber specimens, together with the appearance of the side surface of (a′) $85Al_2O_3$–$15SiO_2$ and (b′) α-Al_2O_3 fibers.

sharp straight-fronted edge notch with a notch-tip radius around 25 nm could be introduced in the polycrystalline (Tyranno-SA®, grade 3, Ube Industries) and amorphous (Tyranno-ZMI®, Ube Industries) SiC fibers. In the present work, as the method to introduce a notch, the FIB method was applied to two types of the alumina fibers ($85Al_2O_3$–$15SiO_2$ fiber, Altex®, Sumitomo Chemical Co., Ltd., where the figure of 85 for Al_2O_3 and that of 15 for SiO_2 refer to the chemical composition in wt %, and α-Al_2O_3 fiber, Almax®, Mitsui Mmining Co., Ltd.).

Fig. 1 shows the fracture surface and side surface of the $85Al_2O_3$–$15SiO_2$ and α-Al_2O_3 fibers. The $85Al_2O_3$–$15SiO_2$ fiber showed mirror, mist and hackle zones in fracture surface but not the α-Al_2O_3 fiber. This means that the mirror zone size method could be applied to the estimation of fracture toughness value of the $85Al_2O_3$–$15SiO_2$ fiber but not to that of the crystalline fiber (α-Al_2O_3). To reveal the fracture toughness values of both fibers, it is needed to apply the common method to both fibers other than the mirror zone size method. The present approach using the FIB-introduced notch makes it possible to estimate the fracture toughness values comprehensively.

The main aims of the present work were (i) to reveal the fracture toughness values of these fibers, (ii) to examine whether the fracture toughness value is dependent on the fiber diameter and notch depth or not, and (iii), based on the obtained fracture toughness values and the strengths of original fibers without notch, to reveal the critical notch depth at the transition from intrinsic defects-induced fracture to notch-induced one, which corresponds to the equivalent size of the intrinsic defects that determine the strength of the original fiber without notch.

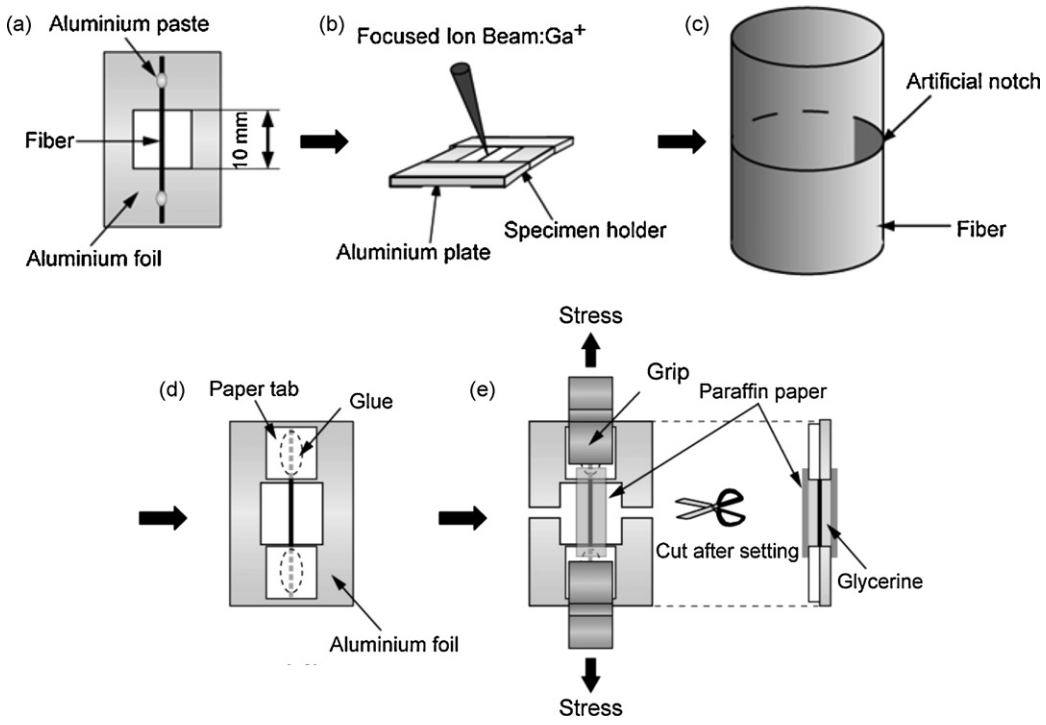

Fig. 2. Procedure (a–c) to introduce an artificial straight-fronted edge notch in fiber specimen and (d and e) to measure the tensile fracture strength.

2. Experimental procedure

2.1. Samples

Two types of the alumina fibers ($85Al_2O_3$–$15SiO_2$ fiber, Altex®, Sumitomo Chemical Co., Ltd., and α-Al_2O_3 fiber, Almax®, Mitsui Mining Co., Ltd) were used for test.

The microstructure of the $85Al_2O_3$–$15SiO_2$ fiber consists of small γ-alumina grains of a few tens of nanometers intimately dispersed in the 15 wt% amorphous SiO_2 phase.[1,2,8] The density has been reported to be 3.2 g/cm^3 and Young's modulus to be 210 GPa.[1,2,8] The average diameter was 17 μm. The fracture surface showed the mirror, mist and hackle zones, as has been shown in (Fig. 1(a)). The side surface was smooth (Fig. 1(a′)). The average strength of the original fiber without notch for a gage length 10 mm was 1.84 GPa, as shown later.

The polycrystalline α-Al_2O_3 fiber used in this work has been known to be composed of almost pure α-alumina.[1,2,9,10] The grain size has been reported to be around 0.5 μm.[1,2,9] The diameter of this fiber is small (around 10 μm), which allows to produce woven cloth from the fiber.[1,2,9,10] The young's modulus has been reported to be 344 GPa.[1,2,9,10] This fiber has lower density of 3.60 g/cm^3 compared to the fully dense α-Al_2O_3 fiber with density 3.92 g/cm^3, and has intragranular porosities.[1,2,9] Actually, in the fracture surface observed in this work, many micro-porosities were found (Fig. 1(b)). The side surface was rather rough (Fig. 1(b′)). The micro-porosities and surface irregularities are considered to act as stress concentration sources, leading to relatively low strength. The average strength of the original fiber without notch for gage length 10 mm was 1.34 GPa, as shown later.

2.2. Introduction of straight-fronted edge notch in fiber test specimens and tensile test

A mode I type straight-fronted edge notch was introduced in each fiber specimen with a FIB-micromachining-method, developed in our preceding work.[13] The outline of the procedure is presented in Fig. 2. First, the fiber was pasted onto a thin aluminum foil with a thickness of 11 μm, as shown in Fig. 2(a). The fiber gage length for tensile testing was 10 mm. The fiber-pasted aluminum foil was placed onto a 0.3 mm thick aluminum plate. The aluminum plate was used as the beam attenuator in the later notch-forming process, and also as the protector from deformation and fracture of fiber specimens in the handling and as the sample carrier. The fiber-pasted aluminum foil and the aluminum plate were wrapped with specimen holders of aluminum, as shown in Fig. 2(b). The assembly was then placed in the FIB apparatus (JFIB-2300, JEOL, Tokyo, Japan). A straight-fronted edge notch (Fig. 2(c)) was introduced in the fiber by the focused Ga^+-ion beam with a 55 nm spot size, at an acceleration voltage of 30 kV and probe current of 80 pA. The fiber diameter D and notch depth a of each test specimen were measured with a scanning ion microscope (SIM) attached to the FIB apparatus.

In preparation for the subsequent tensile testing, a 100 μm thick paper tab was glued to the fiber-ends-area with epoxy resin (High Super 30, Cemedine Co., Ltd., Tokyo, Japan) (Fig. 2(d)) in order to realize higher stress transfer efficiency to the fiber than with the aluminum foil alone. Then, the specimen holder and aluminum plate were removed, and the test specimen shown in Fig. 2(d) was obtained. After placing the test specimen in the tensile machine, the aluminum foil frame was cut so that the applied load was directly applied to the fiber (Fig. 2(e)).

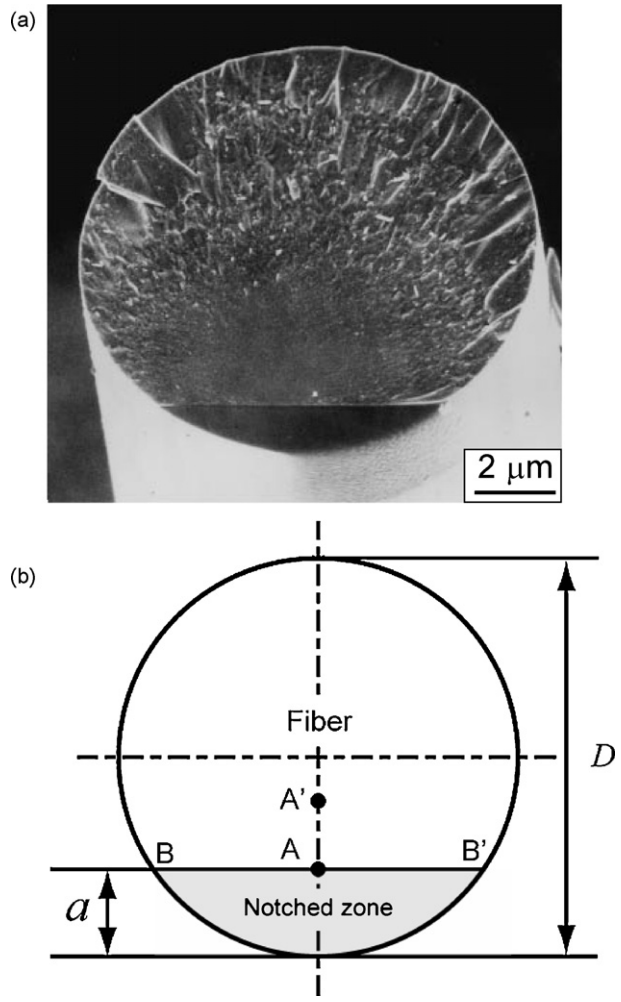

Fig. 3. (a) Fracture surface of the amorphous SiC fiber with a straight-forwarded edge notch introduce with focused-ion-beam, and (b) schematic representation of the fractured fiber cross section. a and D refer to the notch depth and fiber diameter, respectively. The configuration of the mirror, mist and hackle zones in (a) demonstrates that the fiber fracture was caused at A in (b) by the introduced notch and the stress singularity along A–A′ plays a deterministic role in fracture.

Tensile test for the notched and unnotched fiber specimens with a gage length 10 mm was carried out at a crosshead speed of 8.3×10^{-6} m/s at room temperature with a universal tensile testing machine (MMT-10N-2, Shimadzu Co., Kyoto, Japan). The load was monitored with a 2.5 N load cell. In the test, the fiber specimen was wrapped with paraffin papers, in which glycerin was filled in order to prevent the segmentation of the fiber upon fracture, as shown in Fig. 2(e). Thus, the original fracture surface could be obtained for observation. The fracture surface of fibers was observed with a field emission – scanning electron microscope (FE-SEM) (X-500, Toshiba Co., Tokyo, Japan).

2.3. Estimation of fracture toughness value

Fig. 3(a) shows the fracture surface of the amorphous SiC fiber (Tyranno-ZMI®, Ube Industries) with a straight-fronted edge notch introduced with the FIB method, and (b) schematic representation of the fractured fiber cross section, in which the notch depth a and the fiber diameter D are indicated for reference.

The configuration of the mirror, mist and hackle zones in (a) demonstrates that (i) the fiber fracture was caused at A in (b) by the introduced notch and (ii) the stress singularity along A–A′ plays a deterministic role in fracture. (As will be shown later in Section 3.1, the same feature was reconfirmed also from the fracture surface of notched $85Al_2O_3$–$15SiO_2$ fiber specimen (Fig. 5) which showed the mirror, mist and hackles zones similarly to the amorphous SiC fiber). The fracture toughness (K_{Ic}) value was obtained by the following procedure.

The notched strength (the macroscopic fracture stress of the fiber given by the ratio of the fracture force to the fiber cross section) (σ_{FN}), notch depth (a) and fiber diameter (D) were measured for each notched fiber test specimen. According to the fracture mechanics, the fracture toughness K_{Ic} is expressed by[14]

$$K_{Ic} = Y\left[\frac{a}{D}\right]\sigma_{FN}(\pi\alpha)^{1/2} \tag{1}$$

where $Y[a/D]$ is the correction factor for the straight-fronted edge notch in fiber, which is dependent on the relative notch depth a/D. Based on the features (i) and (ii) of fracture morphology mentioned above and the reported result that the $Y[a/D]$ calculated from the stress singularity along A–A′ in Fig. 3(b) for straight-fronted edge crack in a round bar is close to that obtained from the experimental compliance method,[15] the $Y[a/D]$ for the present fiber was calculated also from the stress singularity along A–A′ with a finite element analysis (MARC2001, MSC. Software Corp., USA). The details of the calculation procedure and boundary condition have been shown in our preceding work,[13] in which the $Y[a/D]$ was obtained for SiC fibers. As the elastic properties of the present Al_2O_3 fibers are different from those of SiC ones, the following values were used in the present calculation. The Young's modulus and the Poisson's ratio of the $85Al_2O_3$–$15SiO_2$ fiber were taken from the reported values of 210 GPa[1,2,8] and 0.20,[16] respectively. The Young's modulus of the α-Al_2O_3 fiber was taken from the reported value 344 GPa[1,2,9,10] and the Poisson's ratio from the value of bulk polycrystalline α-Al_2O_3, 0.25.[17] The $Y(a/D)$ for each Al_2O_3 fiber was expressed by

$$\left.\begin{aligned} Y\left[\frac{a}{D}\right] &= 0.99 - 0.61\left(\frac{a}{D}\right) + 5.70\left(\frac{a}{D}\right)^2 - 0.43\left(\frac{a}{D}\right)^3 \quad (85Al_2O_3\text{–}15SiO_2) \\ Y\left[\frac{a}{D}\right] &= 0.98 - 0.87\left(\frac{a}{D}\right) + 9.00\left(\frac{a}{D}\right)^2 - 8.90\left(\frac{a}{D}\right)^3 \quad (\alpha\text{-}Al_2O_3) \end{aligned}\right\} \tag{2}$$

The difference in $Y[a/D]$ between the $85Al_2O_3$–$15SiO_2$ and α-Al_2O_3 fibers stems from the difference in Poisson's ratio.

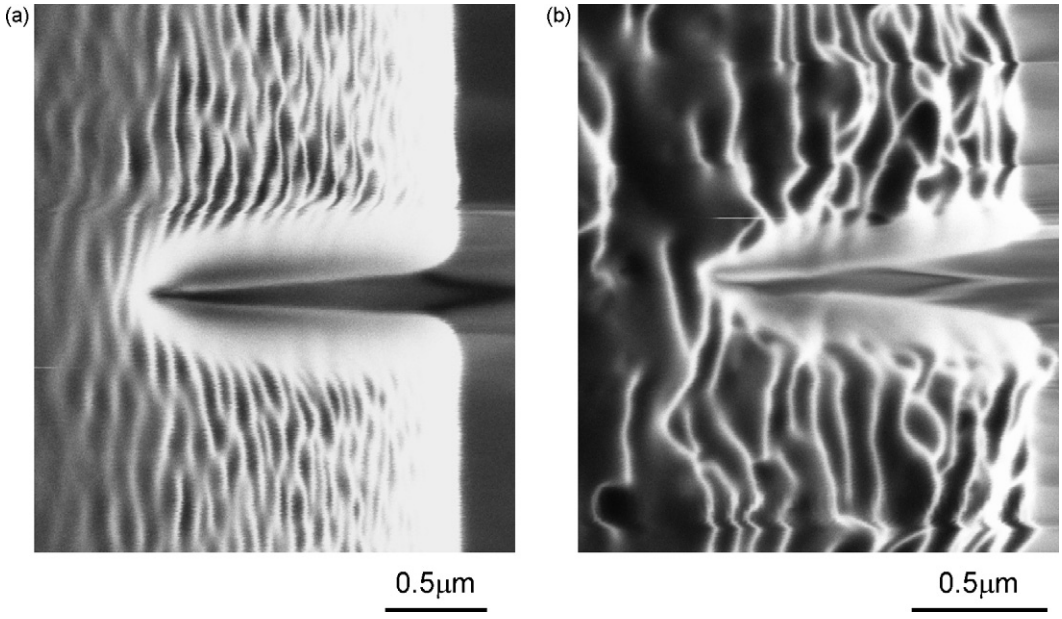

Fig. 4. Appearance of the introduced notch observed from the side surface in (a) the $85Al_2O_3$–$15SiO_2$ and (b) α-Al_2O_3 fiber specimens, observed with SIM, showing the sharp notch front.

Substituting the notched strength (σ_{FN}), notch depth (a) and fiber diameter (D) measured for each fiber test specimen into Eq. (2) and then Eq. (1), we had the fracture toughness value K_{Ic} for each fiber specimen.

3. Results

3.1. Appearance of the introduced notch and fracture surface

Fig. 4 shows the appearance of the introduced notch observed from the side surface in (a) $85Al_2O_3$–$15SiO_2$ and (b) α-Al_2O_3 fiber specimens, observed with SIM. In both fiber specimens, the notch front is sharp. The notch root radius was around 25 nm, as similarly as that observed for amorphous and crystalline SiC fibers.[13] The stress state ahead of the introduced notch is close to that of the cracked case and the finite element calculations in Section 2.3 can be used.

In the fiber surface close to the notch, a wavy pattern was found. Though the reason for this was unknown, it was speculated that the fiber surface close to the notch was etched slightly due to Ga^+ ions. The irregularities caused by the surface etching were, however, far small in comparison with the size of the introduced notch (0.3–2 μm for $85Al_2O_3$–$15SiO_2$ fiber and 0.7–2 μm for α-Al_2O_3 fiber), and the fiber fracture was surely caused by the introduced notch, as shown later in Sections 3.1 and 3.2. In the present work, the influence of the etching of the

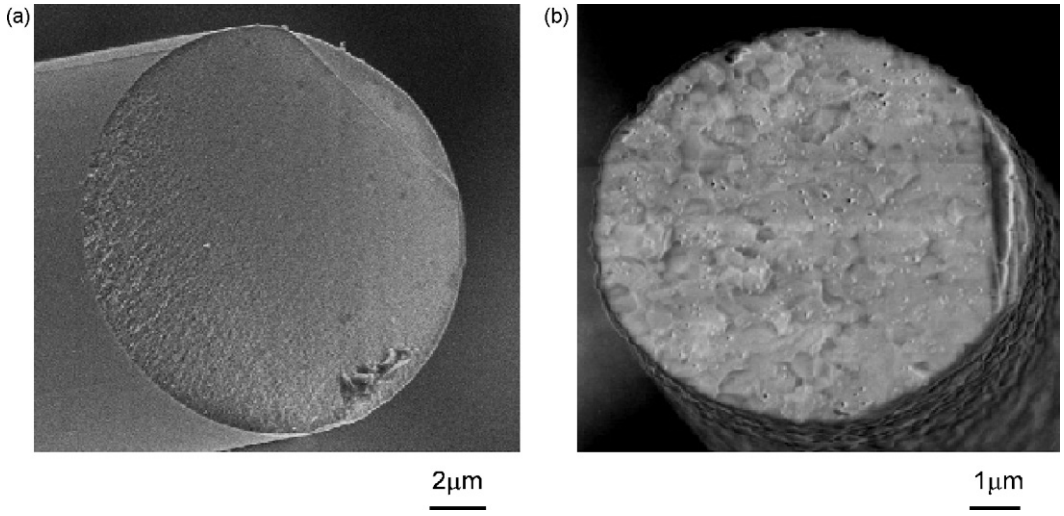

Fig. 5. Fracture surface of the notched (a) $85Al_2O_3$–$15SiO_2$ and (b) α-Al_2O_3 fiber specimens.

Table 1
Measured values of diameter (D), notch depth (a) and fracture strength (<TF), and estimated values of the fracture toughness (K_{Ic}) of 85Ai$_2$O$_3$–15SiO$_2$ and α-Al$_2$O$_3$ fiber specimens.

Sample no.	Diameter D (μm)	Notch depth a (fim)	Fracture strength σ_{FN} (GPa)	Fracture toughness K_{Ic} (MPa m$^{1/2}$)
85Al$_2$O$_3$–15SiO$_2$ fiber				
1	16.7	1.96	0.88	2.15
2	18.4	1.63	0.84	1.87
3	18.7	1.03	0.95	1.66
4	16.2	1.29	0.73	1.44
5	16.4	1.55	1.06	2.29
6	17.1	0.69	1.19	1.70
7	16.3	0.64	1.21	1.67
8	16.6	0.78	1.36	2.07
9	16.7	0.93	1.13	1.88
10	16.4	0.73	1.23	1.82
11	17.4	0.46	1.58	1.85
12	16.9	0.36	1.67	1.73
13	17.5	0.66	1.56	2.18
14	17.5	1.15	0.96	1.78
α-Al$_2$O$_3$ fiber				
1	10.3	1.25	1.01	1.98
2	9.9	1.19	1.02	1.95
3	10.3	1.85	0.88	2.27
4	11.2	1.24	1.06	2.06
5	9.7	1.51	0.98	2.19
6	8.7	1.80	0.72	1.89
7	9.2	0.86	1.35	2.15
8	10.4	1.70	0.86	2.06
9	9.3	0.77	1.25	1.88
10	8.9	0.97	1.21	2.08

fiber surface was neglected in estimation of fracture toughness of the fiber.

Fig. 5 shows the fracture surface of the notched (a) 85Al$_2$O$_3$–15SiO$_2$ and (b) α-Al$_2$O$_3$ fiber specimens. The notched 85Al$_2$O$_3$–15SiO$_2$ fiber specimen (Fig. 5(a)) showed the mirror, mist and hackles zones similarly to the amorphous SiC fiber (Fig. 3(a)). The fracture of the notch-introduced fiber was caused at the center of the notch front (A in Fig. 3(b)). The configuration of the zones indicates that the fracture is determined by the stress singularity ahead of the fracture initiation point (along A–A′ in Fig. 3(b)). In this way, it was reconfirmed that the fracture mechanical approach is applicable to the extension of the notch introduced by the FIB method. As shown in Fig. 5(b), the crystalline α-Al$_2$O$_3$ did not show the amorphous-like fracture patterns, leading it impossible to estimate the fracture toughness value by the mirror zone size method. The introduction of the notch by the present FIB method made it possible to estimate the fracture toughness value for the crystalline fiber. Accordingly, the fracture toughness of both Al$_2$O$_3$ fibers could be estimated comprehensively by this method.

3.2. Fracture toughness values and their dependence on fiber diameter and notch depth

In the test, the fracture surfaces of all notched specimens were observed and it was checked either of the introduced notch or the intrinsic defects caused the fracture. Only the test results of the

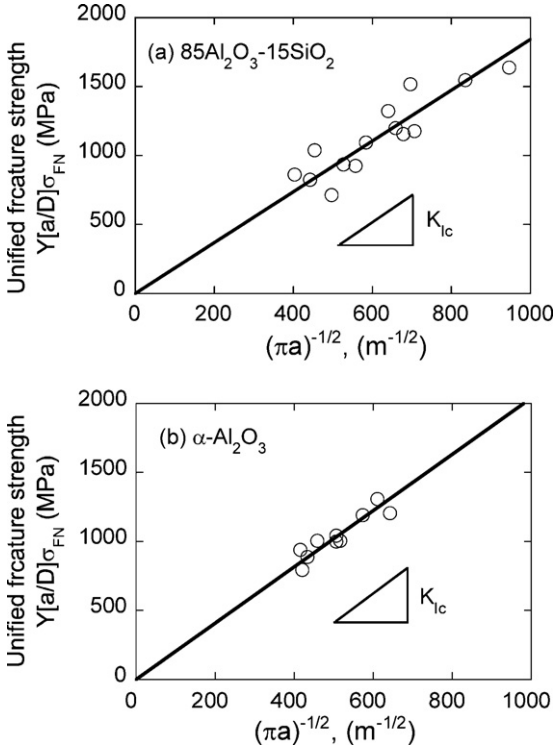

Fig. 6. Unified notch-fracture strength $Y[a/D]\sigma_{FN}$ plotted against $(\pi a)^{-1/2}$.

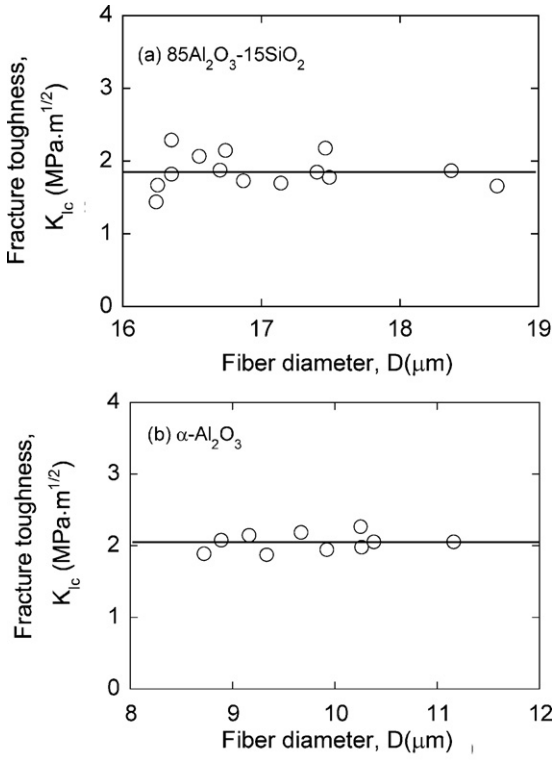

Fig. 7. Estimated fracture toughness (K_{Ic}) values plotted against fiber diameter D for (a) $85Al_2O_3$–$15SiO_2$ and (b) α-Al_2O_3 fiber specimens.

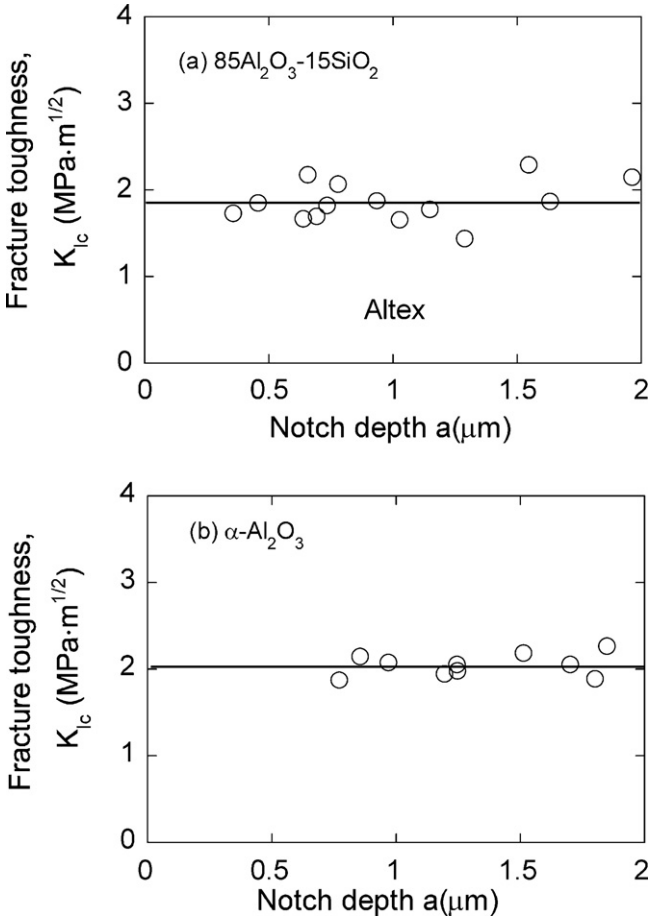

Fig. 8. Estimated fracture toughness (K_{Ic}) values plotted against notch depth a for (a) $85Al_2O_3$–$15SiO_2$ and (b) α-Al_2O_3 fiber specimens.

fiber specimens that were fractured by the introduced notch were used for estimation of the fracture toughness. The measured values of the diameter (D), notch depth (a), fracture strength σ_{FN} and the estimated fracture toughness (K_{Ic}) of the fiber specimens that were fractured by the introduced notch are tabulated in Table 1. The fracture toughness values of the $85Al_2O_3$–$15SiO_2$ with diameter 16.2 –18.7 μm and α-Al_2O_3 fibers with diameter 8.9–11.2 μm were 1.86 ± 0.24 and 2.05 ± 0.13 MPa $m^{1/2}$, respectively.

If the fiber diameter is unique, $Y[a/D]$ given by Eq. (2) can be expressed as a function only of a. However, it was not the present case. Thus even for a given a-value, the K_{Ic}-value given in Eq. (1) becomes different for different diameter. In the present work, we took $Y[a/D]\sigma_{FN}$ as a unifying fracture strength parameter, which is expressed by $Y[a/D]\sigma_{FN} = K_{Ic}\ (\pi a)^{-1/2}$ from Eq. (1). In this expression, $Y[a/D]\sigma_{FN}$ is linearly proportional to $(\pi a)^{-1/2}$ with a slope K_{Ic}. In order to examine whether such a fracture mechanical relation is held or not in the present result, the unifying fracture strength parameter $Y[a/D]\sigma_{FN}$, obtained for each fiber test specimen, was plotted against $(\pi a)^{-1/2}$. The result is presented in Fig. 6. The experimental result of $Y[a/D]\sigma_{FN}$ increases linearly with increasing $(\pi a)^{-1/2}$, indicating that fracture mechanical relation is held for the present notched fiber specimens. The slope corresponds to the fracture toughness value ($K_{Ic} = 1.86$ and 2.05 MPa $m^{1/2}$ for $85Al_2O_3$–$15SiO_2$ and α-Al_2O_3 fibers, respectively).

In order to examine whether the toughness values obtained in the present work is affected by the fiber diameter or not, the obtained K_{Ic} values were plotted against the fiber diameter D, as shown in Fig. 7. The present fracture toughness values were almost independent on the fiber diameter for both $85Al_2O_3$–$15SiO_2$ and α-Al_2O_3 fibers. In the indentation fracture test, the case where the toughness value is dependent on the flaw size[11,12] has been reported. In order to examine whether the toughness values obtained in the present work is affected by the notch size or not, the estimated K_{Ic} values were plotted against the notch depth a, as shown in Fig. 8. The present fracture toughness values are almost independent of the notch depth, indicating that the FIB-introduced notch is appropriate for fracture toughness estimation and the obtained toughness value can be used as the material property.

3.3. Change of fracture strength with increasing notch depth, and estimation of critical defect size at transition from the intrinsic defect-induced fracture to artificial notch-induced one

The fracture strengths σ_{F0} of the original fibers without artificial notch, tested for a gage length 10 mm, were 1.84 ± 0.40 and 1.34 ± 0.42 GPa for $85Al_2O_3$–$15SiO_2$ and α-Al_2O_3 fibers, respectively.

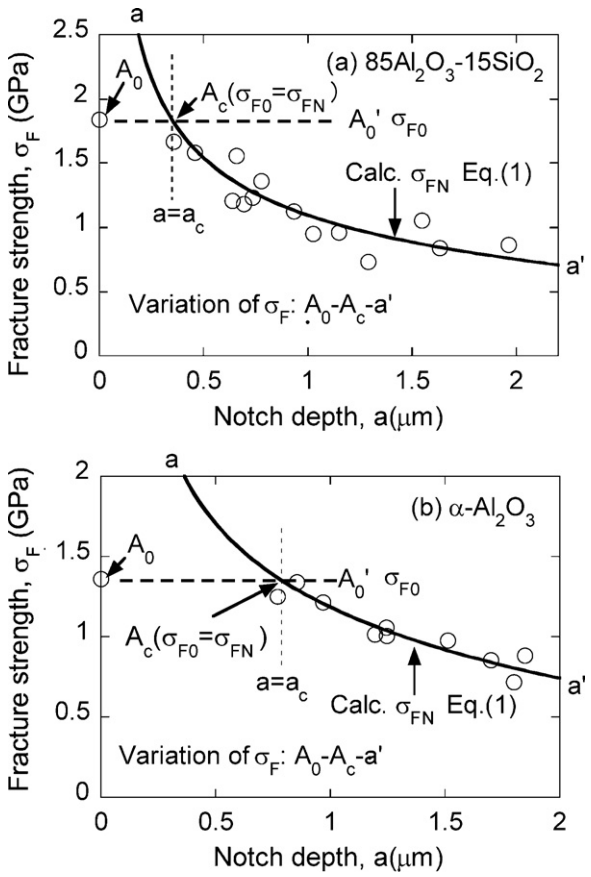

Fig. 9. Measured fracture strength (σ_F) values plotted against the notch depth a for (a) $85Al_2O_3$–$15SiO_2$ and (b) α-Al_2O_3 fibers. The broken line A_0–A_0' shows the original strength σ_{F0} and the solid curve a–a′ shows the change of the notched strength σ_{FN} with notch depth a, calculated by Eq. (1). A_c is the critical point at which $\sigma_{F0} = \sigma_{FN}$ is satisfied. The practical fracture strength σ_F, given by the lower value between σ_{F0} and σ_{FN}, varies with the notch depth a along A_0–A_c–a'. The notch depth a at A_c, a_c (=0.3 and 0.8 μm for $85Al_2O_3$–$15SiO_2$ and α-Al_2O_3 fibers, respectively), refers to the critical notch depth at the transition from the intrinsic defect-induced fracture to the notch-induced one and also to the equivalent size of the intrinsic defects determining the original fiber strength σ_{F0}.

The fracture of the original fiber without notch is caused by the intrinsic defects. In this sub-section, the fracture strength determined by the intrinsic defects is noted as σ_{F0} in order to distinguish from the notched strength σ_{FN} determined by the extension of the notch. As shown below, even a notch is introduced, if the notch depth a is smaller than a critical value a_c, the fracture of the fiber is caused by the intrinsic defects and the practical fracture strength σ_F is given by σ_{F0}. When the notch depth a is larger than a_c, the fracture is caused by the notch extension and the practical fracture strength σ_F is given by σ_{FN}. In this sub-section, using the fracture toughness values obtained in Section 3.2 and the original fiber strength σ_{F0} mentioned above, we revealed the critical notch depth a_c at the transition from the intrinsic defect-induced fracture to artificial notch-induced one and the variation of the fracture strength σ_F with increasing notch depth a for both Al_2O_3 fibers, as follows.

Fig. 9 shows the measured fracture strength (σ_F) values ($\sigma_F = \sigma_{F0}$ for original fibers and $\sigma_F = \sigma_{FN}$ for the notch-fractured fiber specimens) plotted against notch depth a for (a) $85Al_2O_3$–$15SiO_2$ and (b) α-Al_2O_3 fiber specimens. The variation of fracture strength σ_F with notch depth a is described as follows. The broken line A_0–A_0' shows the original strength level (σ_{F0} = 1.84 and 1.34 GPa for $85Al_2O_3$–$15SiO_2$ and α-Al_2O_3 fibers, respectively). The solid curve a–a′ shows the variation of the notched strength σ_{FN} with notch depth a, calculated by Eq. (1) with the measured average values of K_{Ic} = 1.86 MPa $m^{1/2}$ and D = 17.1 μm for $85Al_2O_3$–$15SiO_2$ fiber and K_{Ic} = 2.05 MPa $m^{1/2}$ and D = 9.79 μm for α-Al_2O_3 fiber. The σ_{F0} is lower than σ_{FN} up to the notch depth $a = a_c$ at the cross-point A_c of the σ_{F0}–a and σ_{FN}–a relations, at which σ_{F0} is equal to σ_{FN}. Within the range of $0 \le a \le a_c$, the fiber is fractured by the intrinsic defects in advance of the extension of the introduced notch, and therefore, the fiber strength is kept to be σ_{F0}.[18–20] On the other hand, in the range of $a_c \le$ a, σ_{FN} is lower than σ_{F0}. Accordingly, the fiber is fractured by the introduced notch and its strength is given by σ_{FN}.[18–20] In this way, the fracture strength σ_F is given by the lower value between σ_{F0} and σ_{FN}, and the σ_F varies with a along A_0–A_c–a′.

The A_c shows the critical point at deviation from the intrinsic defect-induced fracture to the notch-induced one. The corresponding notch depth a_c was calculated to be 0.3 and 0.8 μm for $85Al_2O_3$–$15SiO_2$ and α-Al_2O_3 fibers, respectively, by $\sigma_{F0} = \sigma_{FN}$ with the K_{Ic} and D values mentioned above. As $\sigma_{F0} = \sigma_{FN}$ is satisfied at $a = a_c$, the a_c corresponds to the equivalent size of the intrinsic defects that cause the fracture of the original fibers. This means that the average size of the original strength-determining defects was to be around 0.3 and 0.8 μm, respectively. These results suggest that the existent micro-porosities (Fig. 1(b)) and surface irregularities (Fig. 1(b′)) in the α-Al_2O_3 fiber act to reduce the original strength, and due to the reduction in original strength, the notch depth a_c at the transition from intrinsic defect-fracture to notch-fracture is enhanced.

4. Conclusions

(1) The mode I fracture toughness values of the $85Al_2O_3$–$15SiO_2$ (Altex®, Sumitomo Chemical Co., Ltd) and α-Al_2O_3 (Almax®, Mitsui Mining Co., Ltd) fibers were estimated to be 1.86 and 2.05 MPa $m^{1/2}$, respectively, by introducing an artificial straight-fronted edge notch into each test fiber specimen with a focused-ion(Ga^+)-beam-based micromachining method.
(2) The fracture toughness value was almost independent of the fiber diameter and notch depth in both fibers.
(3) From the obtained fracture toughness values and the measured strength of the original fibers without notch, the variation of the average fracture strength with notch depth was revealed. The sizes of the intrinsic defects that determine the strength of the original fiber, corresponding to the transition notch depth from intrinsic defects-induced fracture to notch-induced one, were estimated to be 0.3 and 0.8 μm for $85Al_2O_3$–$15SiO_2$ and α-Al_2O_3 fibers, respectively.

References

1. Bunsell AR, Berger M-H. Fine diameter ceramic fibres. *J Eur Ceram Soc* 2000;**20**(13):2249–60.
2. Berger M-H. Fine ceramic fibers: from microstructure to high temperature mechanical behavior. *Ceram Trans* 2004;**153**:3–26.
3. Dong SM, Chollon G, Labrugre C, Lahaye M, Guette A, Bruneel JL, Couzi M, Naslain R, Jiang DL. Characterization of nearly stoichiometric SiC ceramic fibres. *J Mater Sci* 2001;**36**(10):2371–81.
4. Kumagawa K, Yamaoka H, Shibuya M, Yamamura T. Thermal stability and chemical corrosion resistance of newly developed continuous Si–Zr–C–O tyranno fiber. *Ceram Eng Sci Proc* 1997;**18**:113–8.
5. Yang W, Araki H, Kohyama A, Yu J, Noda T. New tyranno-SA fiber reinforced CVI-SiC/SiC composite. *J Mater Sci Lett* 2002;**21**(18):1411–3.
6. Honjo K. Fracture toughness of PAN-based carbon fibers estimated from strength-mirror size relation. *Carbon* 2003;**41**(5):979–84.
7. Sauder C, Lamon L, Pailler R. The tensile behavior of carbon fibers at high temperatures up to 2400 °C. *Carbon* 2004;**42**(4):715–25.
8. Abe Y, Horikiri S, Fujimura K, Ichiki E. High performance alumina fiber and alumina/aluminum composites. In: Hayashi T, Kawata K, Umekawa S, editors. *Progress in science & engineering of composites*. Japan Soc. Comp. Mater.; 1982. p. 1427–34.
9. Lavaste V, Berger MH, Bunsell AR, Besson J. Microstructure and mechanical characteristics of alpha-alumina fibers. *J Mater Sci* 1995;**30**(17):4215–25.
10. Saitow Y, Iwanaga K, Itou S, Fukumoto T, Utsuno-miya T. Preparation of continuous high purity α-alumina fiber. In: *Proceedings of the 37th International SAMPE Symposium*. 1992. p. 808–19.
11. Jakus K, Ritter JE, Choi SR, Lardner T, Lawn BR. Failure of fused silica fibers with subthreshold flaws. *J Non-Cryst Solids* 1988;**102**(1–3):82–7.
12. Choi SR, Ritter JE, Jakus K. Failure of glass with subthreshold flaws. *J Am Ceram Soc* 1990;**73**(2):268–74.
13. Morishita K, Ochiai S, Okuda H, Ishikawa T, Sato M, Inoue T. Fracture toughness of crystalline silicon carbide fiber (Tyranno-SA3®). *J Am Ceram Soc* 2006;**89**(8):2571–6.
14. Broek D. *Elementary engineering fracture mechanics*. Alphen aan den Rijn, The Netherlands: Sijthoff and Noordhoff International Publishers; 1978. pp. 71–77.
15. Carpinteri A. Stress intensity factors for straight-fronted edge cracks in round bars. *Eng Fract Mech* 1992;**42**(6):1035–40.
16. Daxner T, Rammerstorfer FG, Segurado J, Pettermann HE. Numerical simulation of the creep deformation of MMCs in 4-point bending mode. *J Eng Mater Technol* 2003;**125**(1):50–5.
17. The Ceramic Society of Japan.*Handbook of Ceramics*. 2nd ed. Gihou-do Publishers; 2002. p. 1145–7.
18. Ochiai S, Murakami Y. Tensile strength of composites with brittle reaction zones at interface. *J Mater Sci* 1979;**14**(4):831–40.
19. Ochiai S, Osamura K, Honjo K. Influence of fracture of coating layer on fiber strength. *Mater Sci Eng* 1992;**A154**(2):149–54.
20. Ochiai S, Tanaka M, Hojo M. Mechanical interactions between fiber and cracked coating layer. *Composites Part A* 1999;**30**(4):451–61.